

# The transverse momentum spectrum of low mass Drell-Yan production at next-to-leading order in the parton branching method

A. Bermudez Martinez<sup>1</sup>, P.L.S. Connor<sup>1</sup>, D. Dominguez Damiani<sup>1</sup>,  
L.I. Estevez Banos<sup>1</sup>, F. Hautmann<sup>2,3</sup>, H. Jung<sup>1</sup>, J. Lidrych<sup>1</sup>, A. Lelek<sup>3</sup>,  
M. Mendizabal<sup>1</sup>, M. Schmitz<sup>1</sup>, S. Taheri Monfared<sup>1</sup>, Q. Wang<sup>1,4</sup>,  
T. Wening<sup>1</sup>, H. Yang<sup>1,4</sup>, R. Žlebčík<sup>1</sup>

<sup>1</sup>DESY, Hamburg

<sup>2</sup>RAL, Chilton OX11 0QX and University of Oxford, OX1 3NP

<sup>3</sup>Elementary Particle Physics, University of Antwerp, B 2020 Antwerp

<sup>4</sup>School of Physics, Peking University

## Abstract

The transverse momentum spectrum of low mass Drell-Yan (DY) production at low center-of-mass energies  $\sqrt{s}$  is calculated by applying transverse momentum dependent (TMD) parton distributions obtained from the Parton Branching (PB) evolution method, combined with the next-to-leading-order (NLO) calculation of the hard process in the MC@NLO method. We compare our predictions with experimental measurements at low DY mass, and find very good agreement. In addition we use the low mass DY measurements at low  $\sqrt{s}$  to determine the width  $q_s$  of the intrinsic Gauss distribution of the PB-TMDs at low evolution scales. We find values close to what has earlier been used in applications of PB-TMDs to high-energy processes at the Large Hadron Collider (LHC) and HERA. We find that at low DY mass and low  $\sqrt{s}$  even in the region of  $p_T/m_{DY} \sim 1$  the contribution of multiple soft gluon emissions (included in the PB-TMDs) is essential to describe the measurements, while at larger masses ( $m_{DY} \sim m_Z$ ) and LHC energies the contribution from soft gluons in the region of  $p_T/m_{DY} \sim 1$  is small.

## 1 Introduction

Higher-order perturbative QCD calculations are required for a precise description of Drell-Yan (DY) production [1] measurements in pp collisions at the LHC [2–7]. The production of Z-bosons at transverse momenta smaller than the boson mass ( $p_T < \mathcal{O}(m_Z)$ ) cannot be described by fixed order calculations, but soft gluon resummation to all orders [8–12] is needed, as featured in various analytical TMD resummation methods [13–25] or in parton showers of multi-purpose Monte Carlo (MC) event generators [26–29] matched with higher-order matrix elements [30–35]. In Ref. [36] it was proposed that the Z-boson  $p_T$  spectrum can be accurately evaluated by using the Parton Branching (PB) formulation [37, 38] of

TMD evolution together with NLO calculations of the hard scattering process in the MADGRAPH5\_AMC@NLO [34] framework. The predictions thus obtained were found to be in very good agreement with measurements from ATLAS at  $\sqrt{s} = 8$  TeV [3] and CMS at  $\sqrt{s} = 13$  TeV [7], with modest sensitivity to the non-perturbative (intrinsic- $k_T$ ) part of the TMD distributions [39].

The transverse momentum spectrum of DY production at lower mass  $m_{DY}$  allows one to study in more detail the non-perturbative contribution, as the phase space for perturbative evolution is reduced. However, the measurement of the transverse momentum at low mass of the DY pair is experimentally very challenging, since one has to measure down to low transverse momenta of the decay leptons, where experimental background and misidentification of the DY lepton pairs can be significant. At the LHC the lowest DY mass used for the low transverse momentum spectra ( $p_T \gtrsim 1$  GeV) is  $\sim 46$  GeV [3], while at lower center-of-mass energies DY measurements covering the low  $p_T$  region for lower masses exist from PHENIX [40] at  $\sqrt{s} = 200$  GeV, from R209 [41] at  $\sqrt{s} = 62$  GeV, and from NuSea [42,43] and E605 [44] at  $\sqrt{s} = 38.8$  GeV. The description of these measurements is discussed in terms of TMDs in Refs. [17,45,46]. In Ref. [17] these measurements are compared with collinear NLO predictions and significant differences were observed.

In this paper we apply the TMD parton densities obtained using the PB method (fitted [47] to inclusive deep-inelastic scattering (DIS) precision data from HERA) together with an NLO calculation of DY production [34] precisely in the same manner as in Ref. [36], but now to treat low-mass DY production. We first briefly review the main elements of the PB approach (Sec. 2) and the matching of the PB-TMDs with the NLO calculation (Sec. 3). Then we show that these low energy measurements are very well described with the PB-MCatNLO approach in the whole region of  $p_T/m_{DY}$  (in contrast to the observation in Ref. [17]) and discuss the role of the non-perturbative (intrinsic- $k_T$ ) distribution (Sec. 4). We finally give conclusions (Sec. 5).

## 2 Collinear and TMD densities from the PB method

The PB method [37,38] allows evolution equations for collinear and TMD parton distributions to be solved numerically in an iterative procedure, by making use of the concept of resolvable and non-resolvable branchings and by applying Sudakov form factors to describe the evolution from one scale to another without resolvable branching. The method is based on introducing the soft-gluon resolution scale  $z_M$  into the QCD evolution equations to separate resolvable and non-resolvable emissions, and treating them via, respectively, the resolvable splitting probabilities  $P_{ba}^{(R)}(\alpha_s, z)$  and the Sudakov form factors

$$\Delta_a(z_M, \mu^2, \mu_0^2) = \exp \left( - \sum_b \int_{\mu_0^2}^{\mu^2} \frac{d\mu'^2}{\mu'^2} \int_0^{z_M} dz z P_{ba}^{(R)}(\alpha_s(\mu'), z) \right) .$$

Here  $a, b$  are flavor indices,  $\alpha_s$  is the strong coupling,  $z$  is the longitudinal momentum splitting variable, and  $z_M < 1$  is the soft-gluon resolution parameter. The PB method is described

in detail in Refs. [38, 47].

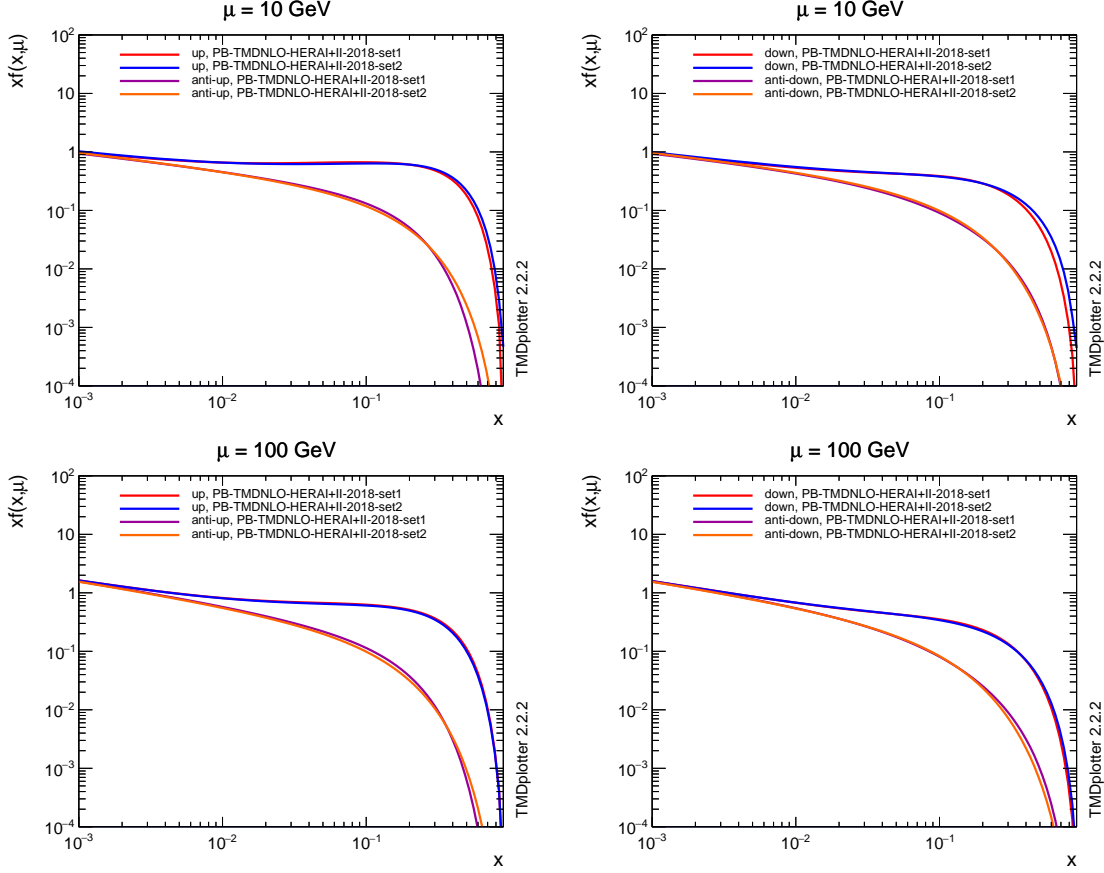


Figure 1: Collinear parton distributions for up and down quarks (PB-NLO-2018-Set1, PB-NLO-2018-Set 2 and NNPDF3.0 [48]) as a function of  $x$  at  $\mu = 10$  and  $100$  GeV.

The TMD parton density distributions are obtained from convolving the evolution kernels  $\mathcal{K}_{ba}$ , given in terms of the splitting functions  $P_{ba}^{(R)}$ , Sudakov form factors  $\Delta_a$  and phase space constraints, with the non-perturbative starting distributions  $\mathcal{A}_{0,b}(x', k_{T,0}^2, \mu_0^2)$ . As described in [47], we have

$$\begin{aligned}
 x\mathcal{A}_a(x, k_T^2, \mu^2) &= x \int dx' \int dx'' \mathcal{A}_{0,b}(x', k_{T,0}^2, \mu_0^2) \mathcal{K}_{ba}(x'', k_{T,0}^2, k_T^2, \mu_0^2, \mu^2) \delta(x'x'' - x) \\
 &= \int dx' \mathcal{A}_{0,b}(x', k_{T,0}^2, \mu_0^2) \frac{x}{x'} \mathcal{K}_{ba}\left(\frac{x}{x'}, k_{T,0}^2, k_T^2, \mu_0^2, \mu^2\right). \quad (1)
 \end{aligned}$$

In general, the starting distribution  $\mathcal{A}_0$  can have flavor-dependent and  $x$ -dependent  $k_{T,0}$  distributions. However, for maximal simplicity we use here a factorized form,

$$\mathcal{A}_{0,b}(x, k_{T,0}^2, \mu_0^2) = f_{0,b}(x, \mu_0^2) \cdot \exp(-|k_{T,0}^2|/\sigma^2)/(\sigma\sqrt{2\pi}) , \quad (2)$$

in which the intrinsic  $k_{T,0}$  distribution is given by a Gauss distribution with  $\sigma^2 = q_s^2/2$  for all parton flavors and all  $x$ , with a constant value  $q_s = 0.5$  GeV. Also, the evolution kernels  $\mathcal{K}_{ba}$  in Eq. (1) do not include any non-perturbative component. In principle, non-perturbative contributions to Sudakov form factors could be introduced in the  $\mathcal{K}_{ba}$  kernels of the PB method, and parameterized in terms of non-perturbative functions to be fitted to experimental data (similarly to what is done in other approaches, e.g. [19–22]). For simplicity, however, at present we take the kernels  $\mathcal{K}_{ba}$  to be purely perturbative.

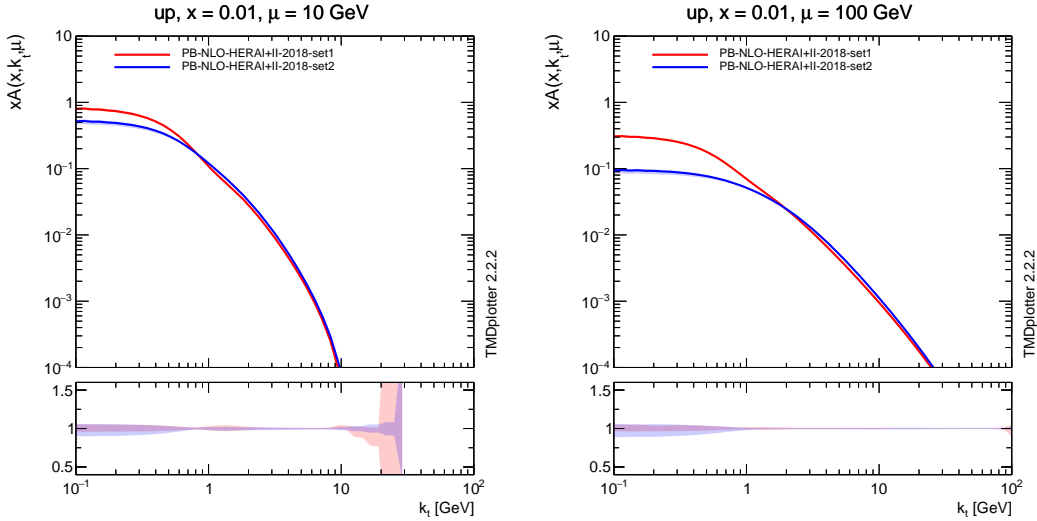


Figure 2: TMD parton distributions for up quarks (PB-NLO-2018-Set1 and PB-NLO-2018-Set 2) as a function of  $k_T$  at  $\mu = 10$  and  $100$  GeV and  $x = 0.01$ . In the lower panels show the full uncertainty of the TMDs, as obtained from the fits [47].

The PB method enables the explicit calculation of the kinematics at every branching vertex, once the evolution scale is specified in terms of kinematic variables. In Ref. [37] it was pointed out that angular ordering gives transverse momentum distributions which are stable with respect to variations of the resolution parameter  $z_M$ . In angular ordering, the angles of the emitted partons increase from the hadron side towards the hard scattering [49, 50]. The transverse momentum of the  $i$ 's emitted parton  $q_{t,i}$  can be calculated in terms of the angle  $\Theta_i$  of the emitted parton with respect to the beam directions from  $q_{t,i} = (1 - z_i)E_i \sin \Theta_i$ . Associating the "angle"  $E_i \sin \Theta_i$  with  $\mu_i$  gives

$$q_{t,i}^2 = (1 - z_i)^2 \mu_i^2 . \quad (3)$$

Collinear and TMD parton distributions were obtained in [47] from fits of the parameters of the starting distributions at scale  $\mu_0 \sim 1$  GeV to the inclusive-DIS precision measurements from HERA, after PB evolution and convolution with the DIS hard-scattering coefficient functions at NLO. The fits were performed using the open-source fitting platform `xFitter` [51] and a new development described in Ref. [38,47] of the numerical techniques [52]. Collinear and TMD distributions were extracted including the determination of experimental and theoretical uncertainties. Two different sets of parton distributions were obtained: Set 1, which corresponds at collinear level to HERAPDF 2.0 NLO [53], and Set 2, which differs by the choice of the scale used in the running coupling  $\alpha_s$ , namely, it uses the transverse momentum (instead of the evolution scale), corresponding to the angular-ordering approach. For soft gluon resolution  $z_M \rightarrow 1$  and strong coupling  $\alpha_s \rightarrow \alpha_s(\mu'^2)$  it was verified [38,47] numerically, with a numerical accuracy of better than 1 % over a range of five orders of magnitude both in  $x$  and in  $\mu$ , that DGLAP evolution equations [54–57] are recovered from PB evolution.

In Fig. 1 the Set 1 and Set 2 collinear densities are shown for up-quark and down-quark at evolution scales of  $\mu = 10$  and 100 GeV. The plots in Figs. 1,2 are made using the TMDplotter tool [58,59]. Collinear densities are available in a format compatible with the one employed in LHAPDF [60], and can be used in calculations of physical processes at NLO.

In Fig. 2 we show the TMD distributions for up-quarks at  $x = 0.01$  and  $\mu = 10$  and 100 GeV.

### 3 PB-TMDs and DY production at NLO

In this section we employ the approach proposed in Ref. [36] to perform the matching of PB-TMDs with the NLO calculation of DY production. We briefly describe a few technical aspects of the computation and analyze numerically the contributions of PB-TMDs and NLO in the matching procedure.

Following [36], we use `MADGRAPH5_AMC@NLO` (version 2.6.4, hereafter labelled `MC@NLO`) [34] and apply the NLO PB parton distributions with  $\alpha_s(M_Z) = 0.118$  for the NLO calculations of inclusive Drell-Yan production. As in [36], motivated by the angular ordering in PB evolution, we use `HERWIG6` [61,62] subtraction terms in `MC@NLO`.

In order to avoid double counting between the contribution of the real emission treated by the matrix element calculation and the contribution from the PB-TMD (which in this respect plays a role analogous to that of parton showers), a matching scale  $\mu_m$  needs to be defined. This scale is determined by the NLO calculation and is transferred to the user via the parameter `SCALUP` (included in the LHE file).

The PB-TMDs depend, as indicated in Eq. (1), on the longitudinal momentum fraction  $x$ , the factorization scale  $\mu$  and the transverse momentum  $k_T$ . The factorization scale  $\mu$  and the longitudinal momentum fraction  $x$  are used in the calculation of the hard process for collinear kinematics and a scale corresponding to  $\mu = \frac{1}{2} \sum_i \sqrt{m_i^2 + p_{t,i}^2}$  is chosen by default, with the sum running over all final state particles, that is, in the case of DY production, over

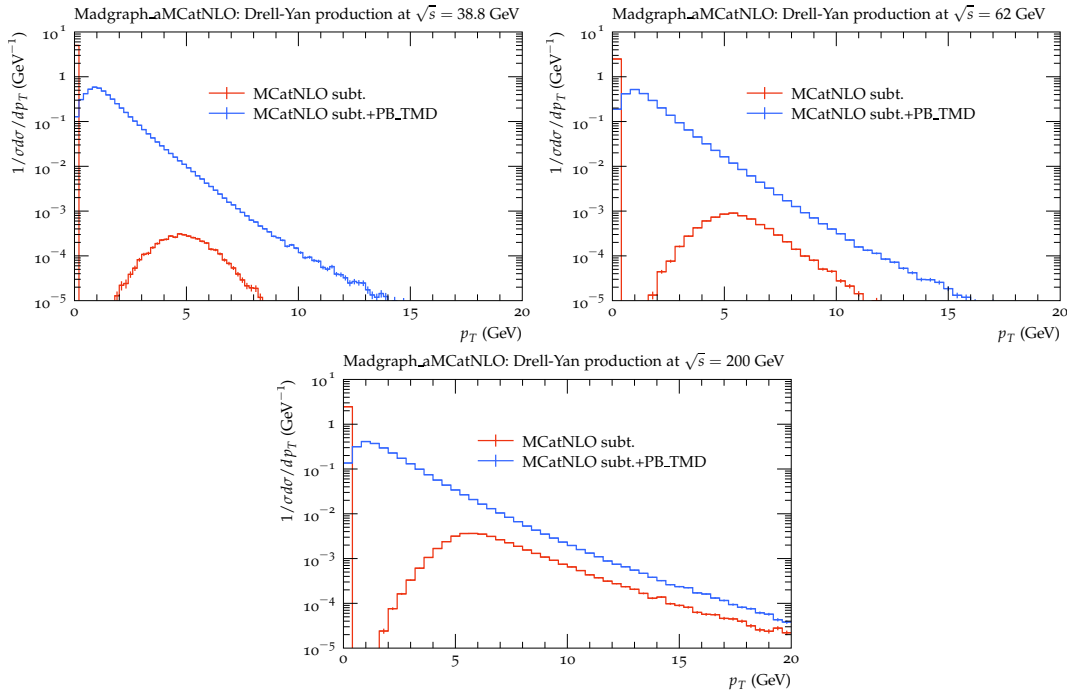


Figure 3: Transverse momentum spectrum of DY production at parton level (LHE level) for subtraction terms and after inclusion of PB-TMDs. Distributions are shown for  $m_{\text{DY}} > 4$  GeV at  $\sqrt{s} = 38.8$  GeV, at  $\sqrt{s} = 62$  GeV and at  $\sqrt{s} = 200$  GeV.

the decay products and the final jet.

In order to allow the full phase space to be covered for the transverse momentum in the PB-TMD, the factorization scale  $\mu$  is set to the invariant mass of the hard process  $\mu = \sqrt{\hat{s}}$  for the underlying Born configuration. For the real emission configuration the scale is changed to  $\mu = \frac{1}{2} \sum_i \sqrt{m_i^2 + p_{t,i}^2}$ , as in the MC@NLO calculation. Finally, the transverse momentum is constrained to be smaller than the matching scale  $\mu_m = \text{SCALUP}$ . The calculation are performed with the CASCADE3 package [63,64] (version 3.0.X), which allows us to read LHE files and to produce output files to be analyzed with Rivet [65].

In Fig. 3 we show results, at different center-of-mass energies  $\sqrt{s}$ , for the DY lepton-pair transverse momentum distribution, obtained from the MC@NLO calculation at a purely partonic level (LHE level) using HERWIG6 subtraction terms (red solid curves in the plots), and from the MC@NLO calculation after inclusion of PB-TMDs (blue solid curves). It is interesting to observe that the contribution coming from the real hard partonic emission is small at low center-of-mass energies and at low  $p_T$ , but increases with increasing  $\sqrt{s}$ , thus allowing one to study the contribution of multiple soft emissions in detail.

In Fig. 4 the distribution in transverse momentum, with subtraction terms and after in-

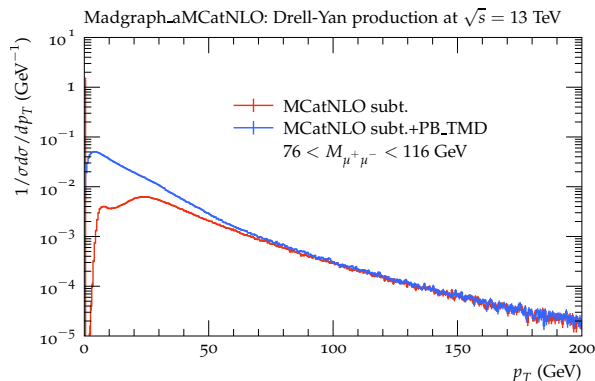


Figure 4: Transverse momentum spectrum of Z production at parton level (LHE level) for subtraction terms and after inclusion of PB-TMDs at  $\sqrt{s} = 13$  TeV.

clusion of PB-TMDs, is shown for LHC energies of  $\sqrt{s} = 13$  TeV and for DY masses around the Z-mass. At high  $\sqrt{s} = 13$  TeV and at sufficiently large DY mass, the predictions with and without PB-TMDs become similar at large transverse momenta, supporting the simple expectation that for  $p_T/m_{\text{DY}} \gtrsim 1$  the transverse momentum spectrum is essentially driven by hard real emission.

## 4 Low mass DY production

We next apply the framework described in the previous section, based on the matching of PB-TMDs with NLO, to the evaluation of DY spectra at low DY masses.

### 4.1 Mass and transverse momentum spectra

We start with the DY mass spectrum at low masses and low  $\sqrt{s}$ . In Fig. 5 we present theoretical predictions obtained from PB-TMDs and NLO matrix elements using MC@NLO matching, and compare them with experimental measurements for different center-of-mass energies from NuSea [42, 43], R209 [41] and PHENIX [40]. We also show the theoretical uncertainties coming from the determination of the PB-TMDs as well as from the variation of the scale in the perturbative calculation. As already observed in Ref. [36] for the case of Z-production at the LHC, the contribution to uncertainties from the parton density turns out to be small compared to the one from the scale uncertainty. Not included are the uncertainties coming from the variation of the intrinsic Gauss distribution ( $q_s$ ), as this parameter was not constrained by the fits to HERA data [47]. This will be further discussed in Subsec. 4.2.

The mass spectra in Fig. 5 are generally well described by the PB-TMD + NLO calculation. For the region of highest masses at lowest  $\sqrt{s}$  (NuSea experiment), we see in the top left panel of Fig. 5 that the description of experimental data by the PB-TMD + NLO calculation

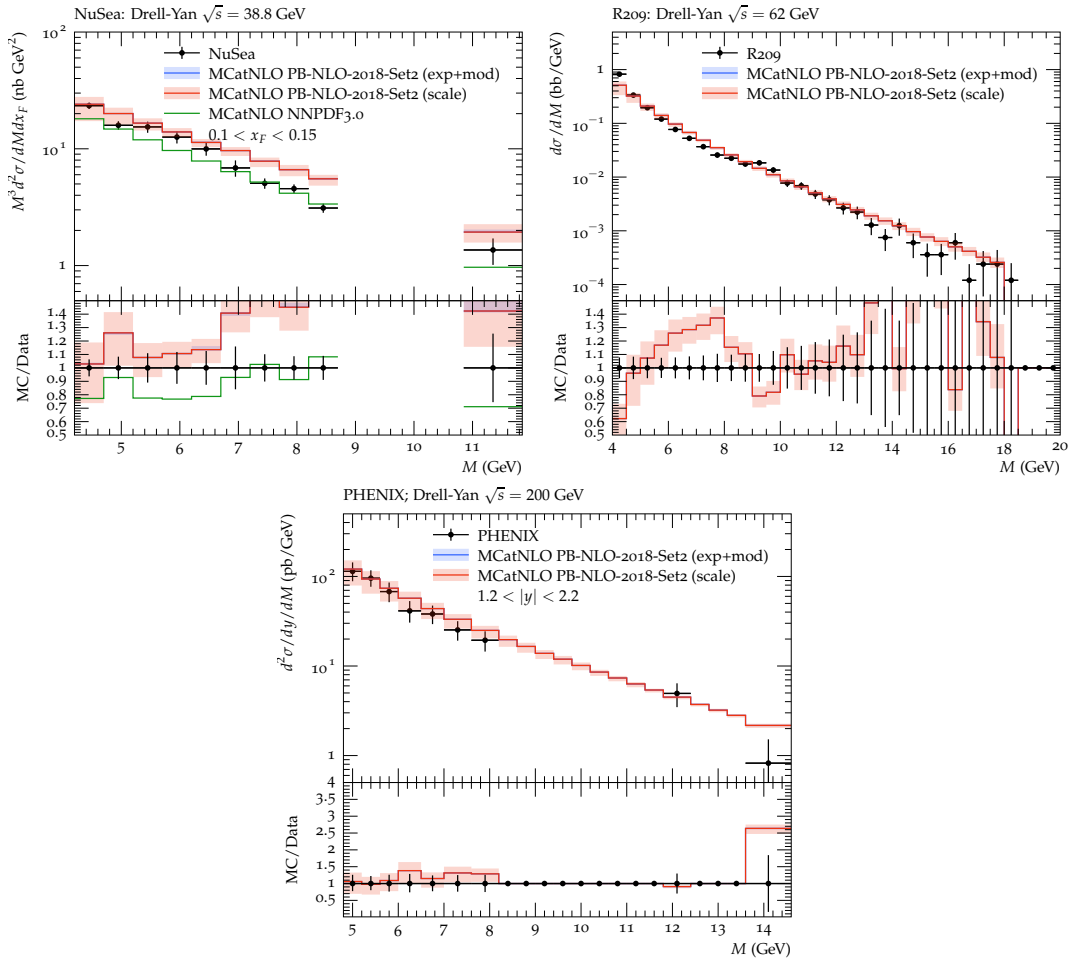


Figure 5: Drell-Yan mass distribution production measured by NuSea [42, 43], R209 [41] and PHENIX [40] compared to predictions at NLO using PB-TMDs. For NuSea also the prediction using NNPDF3.0 [48] is shown.

deteriorates. This is because we enter the large- $x$  region where the parton densities [47] used in the calculation, which are determined from fits to HERA data [53], are poorly constrained. The description in this region can be readily improved by using parton density sets from global fits. We show this in Fig. 5 by plotting the result from the set NNPDF3.0 [48], obtained from global fits that include NuSea data [42, 43]. On the other hand, for the lowest mass region  $m_{\text{DY}} < 6$  GeV of NuSea the mass spectrum is well described. We use this region to investigate the transverse momentum spectrum.

In Fig. 6 we present theoretical predictions from PB-TMDs and NLO matrix elements for transverse momentum spectra, and again we compare them with experimental measure-



ments for different center-of-mass energies from NuSea [42, 43], R209 [41] and PHENIX [40]. The PB-TMDs used in the calculation include an intrinsic (non-perturbative) transverse momentum spectrum parameterized as a Gauss distribution with width  $\sigma^2 = q_s^2/2$  (see eq.(2)). The quality of the description of the measurements (including independent variations of

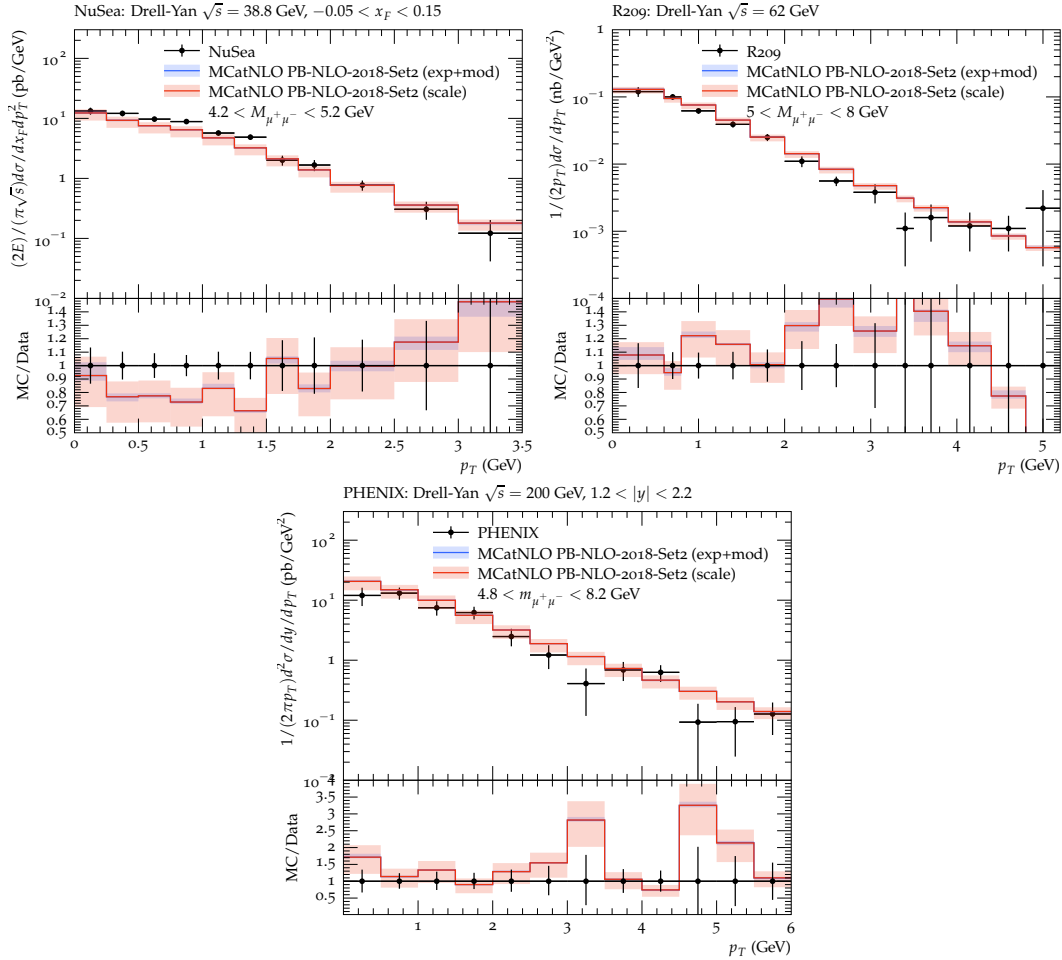


Figure 6: Transverse momentum spectrum of Drell-Yan production measured by NuSea [42, 43], R209 [41], PHENIX [40] compared to predictions at NLO using PB-TMDs.

the factorization and renormalization scales by a factor of two up and down) is good with  $\chi^2/ndf = 1.08, 1.27, 1.04$  for NuSea, R209 and PHENIX, respectively.

In Fig. 7 we show the transverse momentum spectrum of Z-bosons at LHC energies of  $\sqrt{s} = 13$  TeV as measured by CMS [7] and compare it with predictions using the same method of the above low-energy predictions and of Ref. [36], with the PB-TMD Set 2. We observe a very good description of the measurement (with  $\chi^2/ndf = 0.8$  for  $p_T < 80$  GeV).

The drop in the prediction at large transverse momenta comes from missing higher order contributions in the hard process calculation, as discussed in Ref. [36].

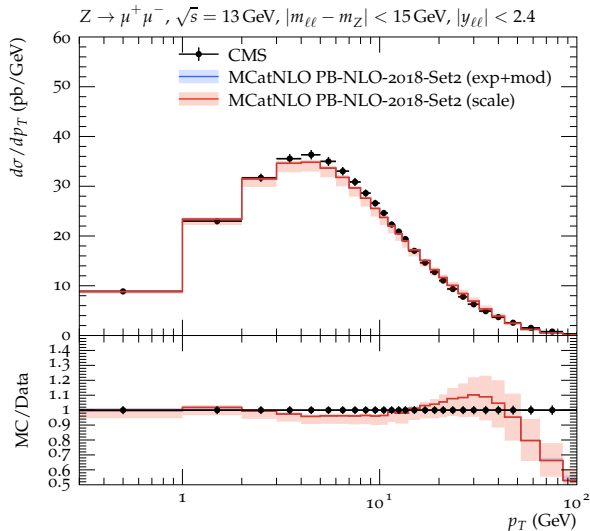


Figure 7: Transverse momentum spectrum of Z production measured by CMS [7] compared to predictions at NLO using PB-TMDs.

## 4.2 Determination of the non-perturbative (intrinsic) transverse momentum distribution

The low-mass DY measurements can be used to constrain the intrinsic transverse momentum distribution. In Fig. 8 we report the calculated  $\chi^2/ndf$  as a function of  $q_s$  obtained from the transverse momentum distributions of NuSea [42, 43], R209 [41], PHENIX [40] (as shown in Fig. 6). For the calculation of  $\chi^2/ndf$  we use the full experimental uncertainties (except an overall normalization uncertainty) and the central values for the theory predictions (without inclusion of pdf and scale uncertainties, leading to a larger  $\chi^2/ndf$  as the one reported in the previous subsection).

A clear minimum is found for NuSea and R209 measurements, with values of  $q_s \sim 0.3 - 0.4$  GeV. On the other hand, the PHENIX measurement shows little sensitivity to the choice of  $q_s$ , which is understandable since only two values for  $p_T < 1$  GeV are measured, while the other experiments have a finer binning. It is interesting to note that the values of intrinsic transverse momentum determined from low-mass DY are rather close to the value of  $q_s = 0.5$  GeV that was assumed in PB-Set2 [47], determined from fits to inclusive DIS data from HERA which are not sensitive to intrinsic- $k_T$ .

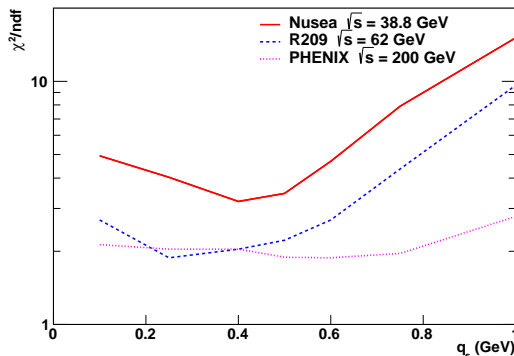


Figure 8: The  $\chi^2/ndf$  as a function of the width of the intrinsic transverse momentum distribution, obtained from a comparison of the measurements (NuSea [42, 43], R209 [41], PHENIX [40]) with a prediction at NLO using PB-TMDs. For the theory prediction only the central value is taken, but no uncertainty from scale variation is included.

### 4.3 Comments on the low-mass region

It has been observed in [17] that NLO calculations in collinear factorization are not able to describe the measurements of DY transverse momentum spectra at fixed-target experiments in the region  $p_T/m_{DY} \sim 1$ . We remark that this is consistent with the observation which we have made in Fig. 3 that, in this kinematic region, the contribution from the real hard emission is small compared to the contribution from multiple parton radiation, embodied in the PB-TMD evolution. Indeed, Fig. 3 indicates that a purely collinear NLO calculation would not give a realistic description of the DY spectrum for  $p_T/m_{DY} \sim 1$  at low energies. On the other hand, Fig. 4 illustrates that the situation is very different at the LHC: in the region around the Z mass shown in Fig. 4, hard real emission dominates the transverse momentum spectrum for  $p_T/m_{DY} \sim 1$ , so that a purely collinear NLO calculation gives a good approximation to the DY process for  $p_T/m_{DY} \sim 1$  at the LHC.

The comparison of theoretical predictions with transverse momentum measurements from NuSea [42, 43] in the top left panel of Fig. 6 confirms that the inclusion of multiple parton emissions, taken into account by the PB-TMD evolution equation [38] (see also discussion in [66]), is essential to describe the region  $p_T/m_{DY} \sim 1$  at low energies. This physical picture is supported by the comparison of theoretical predictions with measurements at the increasingly high energies of R209 [41] and PHENIX [40] in the top right and bottom panels of Fig. 6. Going up to LHC energies in Fig. 7, we see that the PB-TMD + NLO calculation describes the spectrum well all the way up to transverse momenta  $p_T \sim m_{DY}$  (while for even higher  $p_T$  a deficit is observed due to the missing DY + jet NLO correction — see discussion in [36]).

To sum up, the DY transverse momentum in the low-mass region is sensitive to both

finite-order QCD contributions and all-order QCD multi-parton radiation. Theoretical predictions depend on the matching procedure between these contributions. Once this is accomplished, low-mass DY measurements are well described and can provide a wealth of information on non-perturbative QCD dynamics. In this paper the matching is performed, in the spirit of [67], with PB-TMDs and MC@NLO (alternative methods of matching are e.g. those inspired by [12]).

## 5 Conclusion

We have investigated the transverse momentum spectra of DY lepton-pair production at small DY masses and low center-of-mass energies by matching PB-TMD distributions to NLO calculations via MC@NLO. We use the same PB-TMDs and MC@NLO calculations as we have used for Z-production at LHC energies in Ref. [36]. We observe a very good description of the measurements by the NuSea collaboration at  $\sqrt{s} = 38$  GeV, R209 at  $\sqrt{s} = 62$  GeV and PHENIX at  $\sqrt{s} = 200$  GeV, with values of  $\chi^2/ndf \sim 1$  for all measurements. We use the low-mass DY measurements to determine the best value for the width of the intrinsic Gauss distribution, and find a value of  $q_s \sim 0.3 - 0.4$  GeV, slightly smaller than  $q_s = 0.5$  GeV used in the PB-TMD Set 2 distributions [47].

The very good description of low-mass DY measurements is achieved by a combination of a collinear NLO calculation (including the appropriate subtraction terms to avoid double counting) with the PB-TMDs. We find that, at low DY mass and low  $\sqrt{s}$ , even in the region of  $p_T/m_{DY} \sim 1$  the contribution of QCD multi-parton radiation (included in the evolution of PB-TMDs in terms of Sudakov form factors, resolvable splitting functions and phase space constraints) is essential to describe the measurements, while at larger masses ( $m_{DY} \sim m_Z$ ) and LHC energies this contribution is small in the region of  $p_T/m_{DY} \sim 1$ .

**Acknowledgments.** We thank E. Aschenauer, A. Bacchetta, V. Bertone, A. Bressan, M. Dieffenhaller, G. Ferrera and G. Schnell for useful discussions. We thank Yue Hang Leung for discussions on the PHENIX measurement. FH acknowledges the support and hospitality of DESY, Hamburg while part of this work was being done. STM thanks the Humboldt Foundation for the Georg Forster research fellowship and gratefully acknowledges support from IPM.

## References

- [1] S. Drell and T.-M. Yan, “Massive Lepton Pair Production in Hadron-Hadron Collisions at High-Energies”, *Phys.Rev.Lett.* **25** (1970) 316–320.
- [2] CMS Collaboration, “Measurement of the transverse momentum spectra of weak vector bosons produced in proton-proton collisions at  $\sqrt{s} = 8$  TeV”, *JHEP* **02** (2017) 096, arXiv:1606.05864.

- [3] ATLAS Collaboration, “Measurement of the transverse momentum and  $\phi_\eta^*$  distributions of Drell–Yan lepton pairs in proton–proton collisions at  $\sqrt{s} = 8$  TeV with the ATLAS detector”, *Eur. Phys. J.* **C76** (2016), no. 5, 291, arXiv:1512.02192.
- [4] ATLAS Collaboration, “Measurement of the low-mass Drell-Yan differential cross section at  $\sqrt{s} = 7$  TeV using the ATLAS detector”, *JHEP* **06** (2014) 112, arXiv:1404.1212.
- [5] CMS Collaboration, “Measurement of the rapidity and transverse momentum distributions of  $Z$  Bosons in  $pp$  collisions at  $\sqrt{s} = 7$  TeV”, *Phys.Rev.* **D85** (2012) 032002, arXiv:1110.4973.
- [6] ATLAS Collaboration, “Measurement of the transverse momentum distribution of Drell-Yan lepton pairs in proton-proton collisions at  $\sqrt{s} = 13$  TeV with the ATLAS detector”, arXiv:1912.02844.
- [7] CMS Collaboration, “Measurements of differential  $Z$  boson production cross sections in proton-proton collisions at  $\sqrt{s} = 13$  TeV”, *JHEP* **12** (2019) 061, arXiv:1909.04133.
- [8] Y. L. Dokshitzer, D. Diakonov, and S. I. Troian, “On the Transverse Momentum Distribution of Massive Lepton Pairs”, *Phys. Lett.* **B79** (1978) 269–272.
- [9] G. Parisi and R. Petronzio, “Small Transverse Momentum Distributions in Hard Processes”, *Nucl. Phys.* **B154** (1979) 427.
- [10] G. Curci and M. Greco, “Large Infrared Corrections in QCD Processes”, *Phys. Lett.* **92B** (1980) 175–178.
- [11] G. Altarelli, R. K. Ellis, M. Greco, and G. Martinelli, “Vector Boson Production at Colliders: A Theoretical Reappraisal”, *Nucl. Phys.* **B246** (1984) 12–44.
- [12] J. C. Collins, D. E. Soper, and G. F. Sterman, “Transverse Momentum Distribution in Drell-Yan Pair and  $W$  and  $Z$  Boson production”, *Nucl.Phys.* **B250** (1985) 199.
- [13] W. Bizon et al., “Fiducial distributions in Higgs and Drell-Yan production at  $N^3LL+NNLO$ ”, *JHEP* **12** (2018) 132, arXiv:1805.05916.
- [14] W. Bizon et al., “The transverse momentum spectrum of weak gauge bosons at  $N^3LL+NNLO$ ”, arXiv:1905.05171.
- [15] S. Catani, D. de Florian, G. Ferrera, and M. Grazzini, “Vector boson production at hadron colliders: transverse-momentum resummation and leptonic decay”, *JHEP* **12** (2015) 047, arXiv:1507.06937.
- [16] I. Scimemi and A. Vladimirov, “Analysis of vector boson production within TMD factorization”, *Eur. Phys. J.* **C78** (2018), no. 2, 89, arXiv:1706.01473.

- [17] A. Bacchetta et al., “Difficulties in the description of Drell-Yan processes at moderate invariant mass and high transverse momentum”, *Phys. Rev.* **D100** (2019), no. 1, 014018, arXiv:1901.06916.
- [18] A. Bacchetta et al., “Effect of Flavor-Dependent Partonic Transverse Momentum on the Determination of the  $W$  Boson Mass in Hadronic Collisions”, *Phys. Lett.* **B788** (2019) 542–545, arXiv:1807.02101.
- [19] G. Ladinsky and C. Yuan, “The Nonperturbative regime in QCD resummation for gauge boson production at hadron colliders”, *Phys.Rev.* **D50** (1994) 4239, arXiv:hep-ph/9311341.
- [20] C. Balazs and C. P. Yuan, “Soft gluon effects on lepton pairs at hadron colliders”, *Phys. Rev.* **D56** (1997) 5558–5583, arXiv:hep-ph/9704258.
- [21] F. Landry, R. Brock, P. M. Nadolsky, and C. P. Yuan, “Tevatron Run-1  $Z$  boson data and Collins-Soper-Sterman resummation formalism”, *Phys. Rev.* **D67** (2003) 073016, arXiv:hep-ph/0212159.
- [22] P. Nadolsky et al., “The QT resummation portal”.  
<http://hep.pa.msu.edu/resum/>.
- [23] S. Alioli et al., “Drell-Yan production at NNLL'+NNLO matched to parton showers”, *Phys. Rev.* **D92** (2015), no. 9, 094020, arXiv:1508.01475.
- [24] G. Bozzi and A. Signori, “Non-perturbative uncertainties on the transverse momentum distribution of electroweak bosons and on the determination of the  $W$  boson mass at the LHC”, arXiv:1901.01162.
- [25] S. P. Baranov, A. V. Lipatov, and N. P. Zotov, “Drell-Yan lepton pair production at the LHC and transverse momentum dependent quark densities of the proton”, *Phys. Rev.* **D89** (2014), no. 9, 094025, arXiv:1402.5496.
- [26] T. Sjöstrand et al., “An introduction to PYTHIA 8.2”, *Comput. Phys. Commun.* **191** (2015) 159, arXiv:1410.3012.
- [27] J. Bellm et al., “Herwig 7.0/Herwig++ 3.0 release note”, *Eur. Phys. J.* **C76** (2016), no. 4, 196, arXiv:1512.01178.
- [28] M. Bahr et al., “Herwig++: physics and manual”, *Eur.Phys.J.* **C58** (2008) 639–707, arXiv:0803.0883.
- [29] T. Gleisberg et al., “Event generation with SHERPA 1.1”, *JHEP* **0902** (2009) 007, arXiv:0811.4622.
- [30] S. Frixione, P. Nason, and B. R. Webber, “Matching NLO QCD and parton showers in heavy flavour production”, *JHEP* **08** (2003) 007, arXiv:hep-ph/0305252.

- [31] S. Frixione and B. R. Webber, “Matching NLO QCD computations and parton shower simulations”, *JHEP* **0206** (2002) 029, arXiv:hep-ph/0204244.
- [32] S. Frixione, P. Nason, and C. Oleari, “Matching NLO QCD computations with Parton Shower simulations: the POWHEG method”, *JHEP* **0711** (2007) 070, arXiv:0709.2092.
- [33] P. Nason and B. Webber, “Next-to-Leading-Order Event Generators”, *Ann. Rev. Nucl. Part. Sci.* **62** (2012) 187–213, arXiv:1202.1251.
- [34] J. Alwall et al., “The automated computation of tree-level and next-to-leading order differential cross sections, and their matching to parton shower simulations”, *JHEP* **1407** (2014) 079, arXiv:1405.0301.
- [35] R. Frederix et al., “A study of multi-jet production in association with an electroweak vector boson”, *JHEP* **02** (2016) 131, arXiv:1511.00847.
- [36] A. Bermudez Martinez et al., “Production of Z-bosons in the parton branching method”, *Phys. Rev.* **D100** (2019), no. 7, 074027, arXiv:1906.00919.
- [37] F. Hautmann et al., “Soft-gluon resolution scale in QCD evolution equations”, *Phys. Lett.* **B772** (2017) 446, arXiv:1704.01757.
- [38] F. Hautmann et al., “Collinear and TMD quark and gluon densities from Parton Branching solution of QCD evolution equations”, *JHEP* **01** (2018) 070, arXiv:1708.03279.
- [39] R. Angeles-Martinez et al., “Transverse Momentum Dependent (TMD) parton distribution functions: status and prospects”, *Acta Phys. Polon.* **B46** (2015), no. 12, 2501, arXiv:1507.05267.
- [40] PHENIX Collaboration, “Measurements of  $\mu\mu$  pairs from open heavy flavor and Drell-Yan in  $p + p$  collisions at  $\sqrt{s} = 200$  GeV”, *Phys. Rev.* **D99** (2019), no. 7, 072003, arXiv:1805.02448.
- [41] D. Antreasyan et al., “Dimuon Scaling Comparison at 44-GeV and 62-GeV”, *Phys. Rev. Lett.* **48** (1982) 302.
- [42] NuSea Collaboration, “Absolute Drell-Yan dimuon cross sections in 800-GeV/c  $p p$  and  $p d$  collisions”, arXiv:hep-ex/0302019.
- [43] J. C. Webb, “Measurement of continuum dimuon production in 800-GeV/c proton nucleon collisions”, arXiv:hep-ex/0301031.
- [44] G. Moreno et al., “Dimuon production in proton - copper collisions at  $\sqrt{s} = 38.8$ -GeV”, *Phys. Rev.* **D43** (1991) 2815–2836.

- [45] I. Scimemi and A. Vladimirov, “Non-perturbative structure of semi-inclusive deep-inelastic and Drell-Yan scattering at small transverse momentum”, arXiv:1912.06532.
- [46] A. Bacchetta et al., “Transverse-momentum-dependent parton distributions up to  $N^3$ LL from Drell-Yan data”, arXiv:1912.07550.
- [47] A. Bermudez Martinez et al., “Collinear and TMD parton densities from fits to precision DIS measurements in the parton branching method”, *Phys. Rev.* **D99** (2019), no. 7, 074008, arXiv:1804.11152.
- [48] NNPDF Collaboration, “Parton distributions for the LHC Run II”, *JHEP* **04** (2015) 040, arXiv:1410.8849.
- [49] G. Marchesini and B. R. Webber, “Monte Carlo Simulation of General Hard Processes with Coherent QCD Radiation”, *Nucl. Phys.* **B310** (1988) 461.
- [50] S. Catani, B. R. Webber, and G. Marchesini, “QCD coherent branching and semiinclusive processes at large  $x$ ”, *Nucl. Phys.* **B349** (1991) 635–654.
- [51] S. Alekhin et al., “HERAFitter”, *Eur. Phys. J.* **C75** (2015), no. 7, 304, arXiv:1410.4412.
- [52] F. Hautmann, H. Jung, and S. T. Monfared, “The CCFM uPDF evolution uPDFevolv”, *Eur. Phys. J.* **C74** (2014) 3082, arXiv:1407.5935.
- [53] ZEUS, H1 Collaboration, “Combination of measurements of inclusive deep inelastic  $e^\pm p$  scattering cross sections and QCD analysis of HERA data”, *Eur. Phys. J.* **C75** (2015), no. 12, 580, arXiv:1506.06042.
- [54] V. N. Gribov and L. N. Lipatov, “Deep inelastic  $ep$  scattering in perturbation theory”, *Sov. J. Nucl. Phys.* **15** (1972) 438–450. [*Yad. Fiz.*15,781(1972)].
- [55] L. N. Lipatov, “The parton model and perturbation theory”, *Sov. J. Nucl. Phys.* **20** (1975) 94–102. [*Yad. Fiz.*20,181(1974)].
- [56] G. Altarelli and G. Parisi, “Asymptotic freedom in parton language”, *Nucl. Phys.* **B126** (1977) 298.
- [57] Y. L. Dokshitzer, “Calculation of the structure functions for Deep Inelastic Scattering and  $e^+e^-$  annihilation by perturbation theory in Quantum Chromodynamics.”, *Sov. Phys. JETP* **46** (1977) 641–653. [*Zh. Eksp. Teor. Fiz.*73,1216(1977)].
- [58] F. Hautmann et al., “TMDlib and TMDplotter: library and plotting tools for transverse-momentum-dependent parton distributions”, *Eur. Phys. J.* **C 74** (2014), no. 12, 3220, arXiv:1408.3015.



- [59] P. Connor, H. Jung, F. Hautmann, and J. Scheller, “TMDlib 1.0.8 and TMDplotter 2.1.1”, *PoS DIS2016* (2016) 039.
- [60] A. Buckley et al., “LHAPDF6: parton density access in the LHC precision era”, *Eur. Phys. J.* **C75** (2015) 132, [arXiv:1412.7420](#).
- [61] G. Corcella et al., “HERWIG 6.5 release note”, [arXiv:hep-ph/0210213](#).
- [62] G. Marchesini et al., “HERWIG: A Monte Carlo event generator for simulating hadron emission reactions with interfering gluons. Version 5.1 - April 1991”, *Comput. Phys. Commun.* **67** (1992) 465–508.
- [63] H. Jung et al., “The CCFM Monte Carlo generator CASCADE version 2.2.03”, *Eur.Phys.J.* **C70** (2010) 1237, [arXiv:1008.0152](#).
- [64] H. Jung, “The CCFM Monte Carlo generator CASCADE”, *Comput. Phys. Commun.* **143** (2002) 100, [arXiv:hep-ph/0109102](#).
- [65] A. Buckley et al., “Rivet user manual”, *Comput. Phys. Commun.* **184** (2013) 2803–2819, [arXiv:1003.0694](#).
- [66] F. Hautmann, L. Keersmaekers, A. Lelek, and A. M. Van Kampen, “Dynamical resolution scale in transverse momentum distributions at the LHC”, [arXiv:1908.08524](#).
- [67] J. C. Collins and F. Hautmann, “Soft gluons and gauge invariant subtractions in NLO parton shower Monte Carlo event generators”, *JHEP* **0103** (2001) 016, [arXiv:hep-ph/0009286](#).